Studies on Fixed-depth Control of Supercavitating Vehicles

LI Dai-Jin[1] LUO Kai[1] ZHANG Yu-Wen[1] DANG Jian-Jun[1]

Abstract A supercavitating vehicle is a complex high-speed underwater body that is exposed to extreme operating conditions due to its speed. To successfully control the depth and attitude, it is necessary to study the motion characteristics of the vehicles on a vertical plane. This study investigates the motion model on the vertical plane and analyzes the dynamic characteristics of supercavitating vehicles. Then, a fixed-depth control method is developed. For validating the designed control-algorithm, related simulation and experiments have been carried out for the control system. Analytical results show that the proposed control system accomplishes precise depth control of the supercavitating vehicles, providing a necessary theoretical basis for further study of the dynamic control problem for underwater supercavitating vehicles.

Key words Hydrodynamics, supercavitating vehicles, motion characteristics, fixed-depth control

DOI 10.3724/SP.J.1004.2010.00421

When underwater vehicles such as torpedoes and submarines move through water at a sufficiently high speed, the fluid pressure drops locally below the level that sustains the liquid phase and a low-density gaseous cavity forms. Flows exhibiting cavities entirely enveloping the moving body are called "supercavitating"[1]. A schematic diagram of a supercavitating torpedo[2] is shown in Fig. 1.

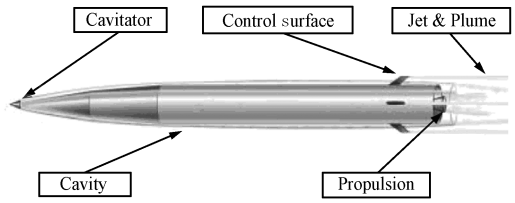

Fig. 1 Schematic diagram of a supercavitating torpedo[3]

In supercavitating flows, the liquid phase does not contact the moving body over most of its length, thus making the skin drag almost negligible. Several new and projected supercavitating underwater vehicles exploit supercavitation as a means to achieve extremely high submerged speeds and low drag[4]. The size of existing or notional supercavitating high-speed bodies ranges from that of a projectile to that of a heavyweight full-scale torpedo[5]. Although extensive efforts have been devoted in the past to the analysis of the fluid dynamic characteristics of supercavitating vehicles[6], very little research has been dedicated so far to the evaluation of the fixed-depth control of slender elastic bodies traveling underwater at high speed in supercavitating regimes. Many of the previous and current studies on guidance, control, and stability have considered supercavitating vehicles as rigid bodies[7−9], while scarcely any have addressed the hydrodynamic characteristics of the water/cavity system[10].

The small wetted-surface area results in a significant reduction of drag. The vehicle may be controlled through a combination of the deflection of the cavitator and control surface, and planning. The control of these bodies presents a number of significant challenges. Depending on the shape of the cavitator, and the size, and immersion of the control surfaces, the body may be inherently stable or unstable. If the body is unstable, active control of the cavitator or control surface in the aft of the vehicle is required to achieve stability[2]. Even if the body is designed to be stable, it is not guaranteed that the vehicle will be stable when in contact with the cavity. Since the cavity wall causes a very large restoring force and the time that the vehicle is in contact with the cavity wall is very short, suppressing these contacts requires very high performance actuators.

The goal of this paper is to investigate the dynamic characteristics of supercavitating bodies, and then to present a fixed-depth control method. The paper is organized as follows. Section 1 outlines the formulation for the motion for the longitudinal or pitch-plane dynamic model. Section 2 describes the considered motion characteristic forces and summarizes the principles of fixed-depth control theory for analysis of the motion stability. Section 3 presents a control algorithm for supercavitating vehicles. Section 4 gives numerical simulation results, and Section 5 carries out experiments for validating the control algorithm, while Section 6 summarizes the main results of the work and gives recommendations for future research.

1 A hydrodynamic and longitudinal kinematics model for a supercavitating vehicle

Although low speed is advantageous for cybernatic and hydrodynamic efficiency, the achievement of high speed for underwater vehicles and projectiles cannot be obtained using conventional hydrodynamics. As a first approximation, underwater supercavitating vehicles can be considered as slender elastic bodies[11]. The nature of the forces acting on a supercavitating vehicle is very complex and still under extensive experimental and numerical investigations. A schematic of the torpedo′s configuration and the applied forces is given in Fig. 2. The body is acted upon by a system of forces corresponding to the interaction of the vehicle′s control surfaces with the cavity boundaries[11]. The control surfaces include the fins at the back of the vehicle and the cavitator, whose primary function is the generation of the supercavity. They support the vehicle in the vertical direction by providing lift and allow maneuvering according to assigned flight paths. Finally, the vehicle′s motion is sustained by a propulsion force. The vehicle interacts with the liquid phase through its front surface (nose or cavitator), beyond which the cavity is formed. The force generated on the cavitator through its interaction with water can be used for controlling the vehicle by orienting the cavitator

Manuscript received August 25, 2008; accepted July 16, 2009
Supported by China Shipbuilding Industry Corporation Foundation (07J4.1)
1. College of Marine Engineering, Northwestern Polytechnical University, Xi′an 710072, P. R. China

at an appropriate angle δ_N. The drag force experienced by the vehicle during its forward motion is given by[12]

$$f_N = \frac{1}{2}\rho A_C C_D(\sigma, 0)V^2 \tag{1}$$

where ρ is the density of the fluid (water), A_C is the cross-section area of the cavitator, and V is the velocity of forward motion of the body. $C_D(\sigma, 0)$ is the cavitator drag coefficient at zero angle of attack, and σ is the cavitation number, which is given by[13]

$$\sigma = \frac{P_\infty - P_c}{\frac{1}{2}\rho v_N^2} \tag{2}$$

where P_∞, P_c are, respectively, the ambient fluid pressure and the vapor pressure in the cavity, v_N is the magnitude of the vehicle velocity at the nose, and ρ is the fluid (water) density. The drag coefficient here is taken to be 0.00805 based on empirical data[14].

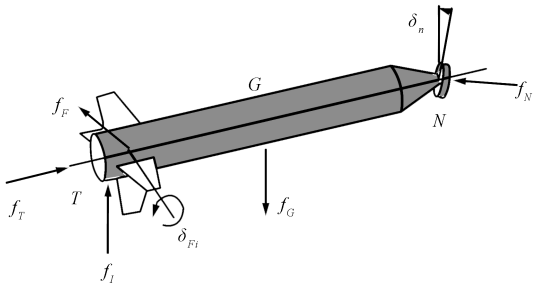

Fig. 2 Configuration of a supercavitating torpedo[11]

The lifting force can be decomposed into three components: force caused by asymmetric supercavitating flow pattern, force acting on the wetted part of the trailing edge, and force caused by angular velocity ω_Z.

The force caused by asymmetric supercavitating flow pattern is the main part of the lifting force. Because of the attack angle α_N, vehicle axis and supercavitating axis are not superposed, and supercavitating flow is in the form of asymmetric flow pattern. The cavity generally surrounds the entire body but may touch the vehicle near the trailing edge or be penetrated by control surface, with the positive attack angle α_N. Because the vehicle is in a gas-filled cavity, there is minimal buoyancy and the weight of the vehicle must be supported on the control surfaces and body. Cavity stability considerations generally require that if the body does touch the cavity, it should be in the region of the trailing edge or transom. The vehicle may be controlled through a combination of the deflection of the cavitator and control surface and planning.

Since the cavity wall causes a very large restoring force and the time that the vehicle is in contact with the cavity wall is very short, suppressing these oscillations requires very high performance actuators.

To derive the equations of motion, the following assumptions are made:

1) The motion of the projectile is confined to a plane;

2) The effect of rolling angular is negligible;

3) The effect of added mass on the dynamics of the projectile is negligible;

4) The motion of the projectile is not influenced by the presence of gas, water vapor, or water drops in the cavity;

5) The velocity and cavitation number are confined to fixed values.

The supercavitating vehicle′s longitudinal plane kinematics equation makes up the system model[15]:

$$mv\dot{\Theta} = A^d k + A^\alpha \alpha + A^\omega \omega_z - G \tag{3}$$

$$J_z\dot{\omega}_z = M^d k + M^\alpha \alpha + M^\omega \omega_z \tag{4}$$

$$\dot{\theta} = \omega_z \tag{5}$$

$$\dot{y} = v\Theta \tag{6}$$

$$\Theta = \theta - \alpha \tag{7}$$

where m is the mass of the vehicle, Θ is the obliquity of the trajectory, θ is the pitch attitude, and J_z is the moment of inertia about z axis. The combined coefficients A^d, A^α, A^ω, M^d, M^α, and M^ω are given by

$$A^d = 0.5C_D^d(\sigma, \alpha_N)\rho A_d v^2 \tag{8}$$

$$A^\alpha = 0.5C_D^\alpha(\sigma, \alpha_N)\rho A_b v^2 \tag{9}$$

$$A^\omega = 0.5C_D^\omega(\sigma, \alpha_N)\rho A_b v^2 \tag{10}$$

$$M^d = 0.5\rho v^2 A_d L m_d^d \tag{11}$$

$$M^\alpha = \begin{cases} 0.5\rho v^2 A_b L m_{bs}^\alpha, |\alpha| \le \alpha_S \\ 0.5\rho v^2 A_b L m_{bB}^\alpha, |\alpha| > \alpha_S \end{cases} \tag{12}$$

$$M^\omega = 0.5m_b^\omega \rho A_b L^2 v \tag{13}$$

In (3) and (4), balanceable angle of attack and balanceable rudder angle can be obtained as follows:

$$\alpha_0 = \frac{GM^d}{A^\alpha M^d - A^d M^\alpha} \tag{14}$$

$$d_0 = -\frac{GM^\alpha}{A^\alpha M^d - A^d M^\alpha} \tag{15}$$

Generally speaking, M^α should be fixed under the condition of $|\alpha| \le \alpha_S$. Because damping derivatives m_{bs}^α is negative near by α_0, the vehicle is statically stable. Although $|\alpha| > \alpha_S$ (For example, the control system of the vehicle dose not work.), m_{bs}^α would become a positive number. The angle of attack decreases monotonously. So the academic minimum d is given by (4).

The angle of nose rudder d should be concerned.

$$d_{\min} = -\frac{M^\alpha}{M^d}\alpha, \quad |\alpha| > \alpha_S \tag{16}$$

It is necessary to investigate the motion characteristics under the condition of $|\alpha| \le \alpha_S$ to control the depth and the attitude.

This part of the paper presents a derivation of a benchmark problem for controlling a supercavitating vehicle. The benchmark problem focuses exclusively on dynamics of a vehicle, which currently appears to present the most severe challenges.

2 Motion characteristics of the vehicles

Under the condition above, the transfer functions of the system can be obtained as

$$\alpha(s) = G(s)\frac{J_z s - M^{\omega}}{\bar{X}(s)} + d(s)\cdot\frac{-A^d J_z s + A^d M^{\omega} - A^{\omega} M^d + mvM^d}{\bar{X}(s)} \quad (17)$$

$$\omega_z(s) = G(s)\frac{M^{\alpha}}{\bar{X}(s)} + d(s)\cdot\frac{mvM^d s + A^{\alpha} M^d - A^d M^{\alpha}}{\bar{X}(s)} \quad (18)$$

$$\theta(s) = \frac{\omega_z(s)}{s} \quad (19)$$

$$y(s) = -v\frac{\theta(s) - \alpha(s)}{s} \quad (20)$$

$$\bar{X}(s) = mvJ_z s^2 + (A^{\alpha} J_z - mvM^{\omega})s + A^{\omega} M^{\alpha} - A^{\alpha} M^{\omega} - mvM^{\alpha} \quad (21)$$

In the functions, the importers are not only d but also G, which is a disturbance quantity.

Although a supercavitating vehicle moves in the cruise phase, G reduces monotonously with the propellant reduction. As G has been neglected in [15], the trajectory of the vehicle slants upward. So the control system in it is not suitable for a large voyage.

G can be labeled as

$$G(s) = \frac{-k_G}{s^2} \quad (22)$$

$$k_G = \dot{m}_f g \quad (23)$$

where g is the acceleration of gravity. In case of a water-ramjet engine, the fuel tank is pressurized by seawater. And k_G is given by

$$k_G = \dot{m}_f g\frac{\rho_f - \rho}{\rho_f} \quad (24)$$

where ρ is the seawater density and ρ_f is the fuel density.

There are two integral actions in the transfer function channel of y to G and one in θ to G. θ and y would change monotonously to respond to G which should be paid full attention in order to guarantee system security.

As an example, a small caliber (about 200 mm) supercavitating vehicle is analyzed.

There is a pair of negative real part poles in the transfer function channel of d to a. The unit step response, which is an insufficient damp oscillation with an overshoot, is presented in Fig. 3. The vehicle gets little added moment of inertia since a majority of its surface is enveloped by supercavitation, which explains the physical phenomenon of the overshoot. This is the greatest dissimilarity from a fully wetted underwater vehicle[14].

In order to avoid the case of $|\alpha| > \alpha_S$, the large overshoot must be considered in control-algorithm design.

There are a pair of negative real part poles and a negative real zero in the transfer function channel of d to ω_z. The unit step response is similar to the channel of α.

There are not only a pair of negative real part poles but also a negative real zero and a negative real zero-pole in the transfer function channel of d to θ. Frequency characterization is shown in Fig. 4. And root locus is shown in Fig. 5. Frequency curve crosses 0 dB line by -20 dB/dec. Both amplitude gain and phase margin are abundant.

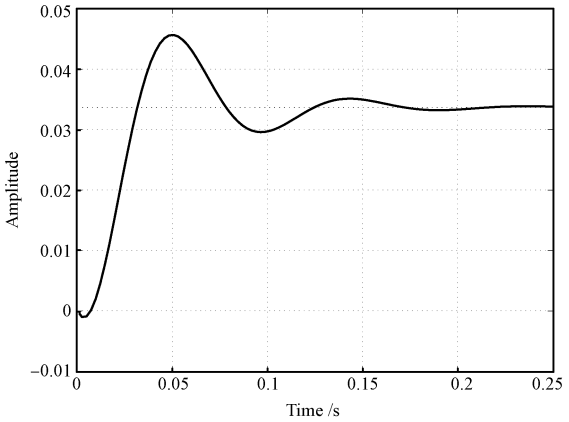

Fig. 3 The unit step response of attack angle

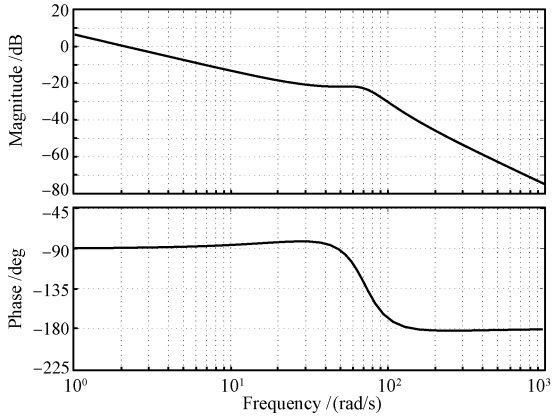

Fig. 4 Frequency characterization of pitch attitude

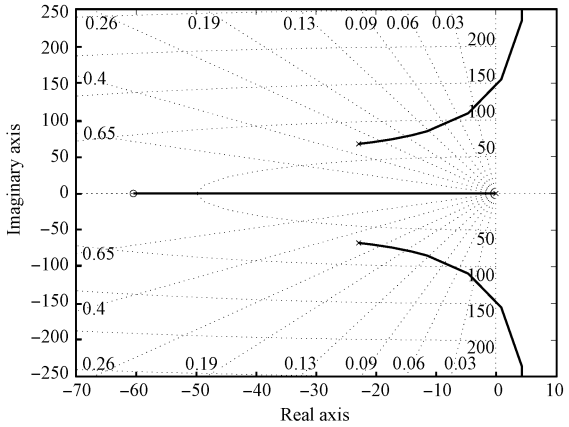

Fig. 5 Root locus of pitch attitude

There are not only a pair of negative real part poles but also a pair of negative real part conjugated zeros and two zero-poles in the transfer function channel of d to y. Frequency characterization is shown in Fig. 6. And root

locus is shown in Fig. 7. Frequency curve crosses 0 dB line by −40 dB/dec. Root locus curve has branches only in the right half plane. There is a couple of integral actions in the forward channel of transfer functions[16].

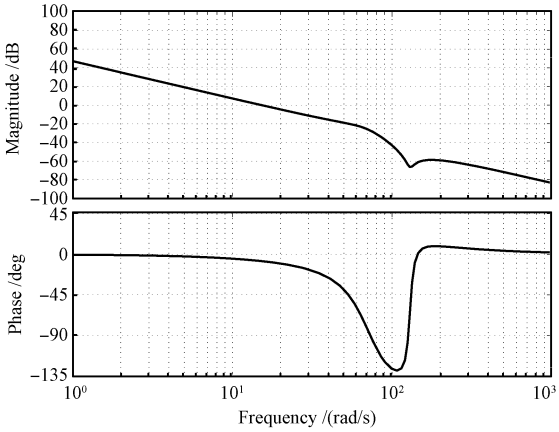

Fig. 6 Frequency characterization of depth

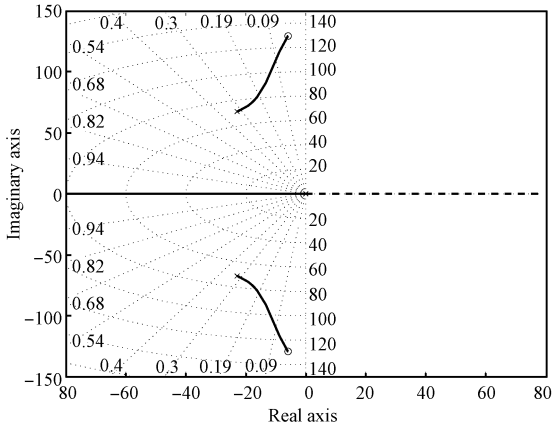

Fig. 7 Root locus of depth

3 The control-algorithm design

Transfer functions of the control system (containing electric actuator) can be expressed as

$$G_c^y(s) = \frac{k(s)}{y_c(s) - y(s)} \tag{25}$$

where y_c is expectant depth. And transfer function of the closed loop is given as

$$y(s) = \frac{1}{\bar{M}_4 s^4 + \bar{M}_3 s^3 + \bar{M}_2 s^2 + 1} y_c(s) + \frac{M^\alpha}{\dfrac{(M^k A^\alpha - M^\alpha A^k) G_c^y(s)}{\bar{M}_4 s^4 + \bar{M}_3 s^3 + \bar{M}_2 s^2 + 1}} G(s) \tag{26}$$

where $\bar{M}$ is a combinatorial coefficient. y is the superposition output responding to both y_c and G. y achieves no-steady-state error tracking responding to y_c. While responding to G which inputs in form of ramp, the steady-state error is given as

$$\lim_{t\to\infty} y(s) = \lim_{s\to 0} \frac{\dfrac{M^\alpha - (J_z s - M^\omega)\, s}{(M^k A^\alpha - M^\alpha A^k)\, G_c^y(s)}}{\bar{M}_4 s^4 + \bar{M}_3 s^3 + \bar{M}_2 s^2 + 1} \frac{k_G s}{s^2} = \lim_{s\to 0} \frac{M^\alpha k_G}{(M^k A^\alpha - M^\alpha A^k)\, G_c^y(s)\, s} \tag{27}$$

Equation (27) tends to infinity, if there is no integral action in $G_c^y(s)$. Therefore, there are two choices to control $G_c^y(s)$: PI or PID.

By controlling $G_c^y(s)$ with PI control method, the transfer function contains a negative real zero and a real zero-pole in the forward channel. Moreover root locus curve would always have two branches in the right half plane, which cannot guarantee system security[17].

By controlling $G_c^y(s)$ with PID control method, the control algorithm is given as

$$G_c^y(s) = k_P + T_D s + \frac{1}{T_I s} \tag{28}$$

where k_P is proportional gain, T_D is differential time, and T_I is integral time. The transfer function contains a negative real zero and a pair of real zero-poles in the forward channel. Root locus curve adjusted is shown in Fig. 8. And frequency characterization is shown in Fig. 9. Amplitude frequency curve crosses 0 dB line by −20 dB/dec. Both amplitude gain and phase margin are abundant.

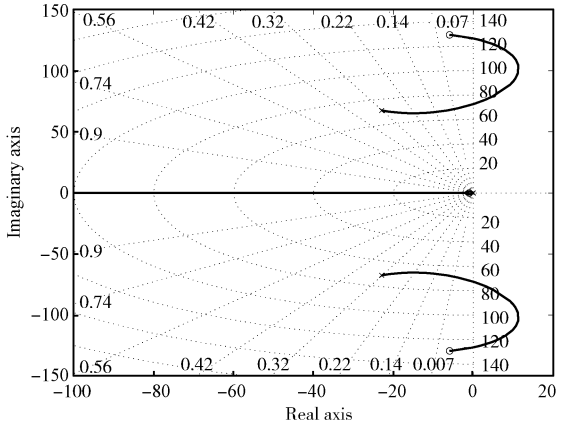

Fig. 8 Root locus of depth by PID control

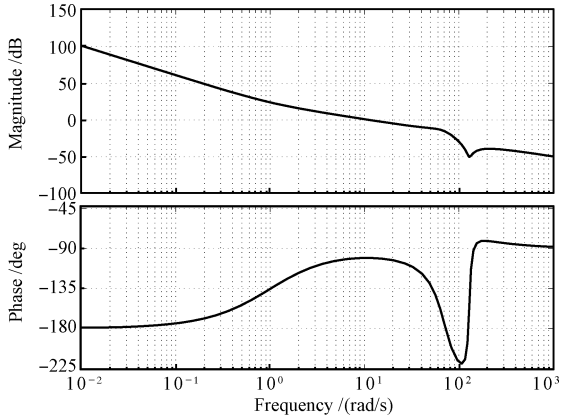

Fig. 9 Frequency of depth by PID control

To simplify the system and get better robustness, the fixed-depth control with limit rudder model should be implemented. From (28), the control algorithm of fixed-depth can be obtained as

$$k_c = k_0 + \Delta k \cdot \mathrm{sgn}\left(k_P \Delta y + T_D \theta + \frac{1}{T_I}\int_0^t \Delta y \mathrm{d}t\right) \quad (29)$$

where k_c represents command angle of the head rudder, k_0 is balanced angle, Δk is change angle, and Δy is depth deviation. In order to reduce the depth deviation, the expectant pitch attitude angle should be set to the estimated value of the balanced attack angle.

In addition, overshoot of step-response system φ is defined because $|\alpha| > \alpha_S$ is not allowed in the control process. The restriction of Δk is as follows:

$$\Delta k \leq \frac{\alpha_s - \alpha_0}{k_{k\alpha} 1 + 2\varphi} \quad (30)$$

4 Numerical simulation

The following values have been used in the numerical simulation:

1) Mass of the vehicle m is 100 kg;
2) Depth of firing beneath the water surface is 2 m;
3) Sailing time is 4 s;
4) Shooting speed is 44 m/s ($t = 0$);
5) When $t = 0.23$ s, the vehicle achieves invariable speed is 203 kN;
6) Thrust of solid rocket motor is 25 kN/0.5 s, and specific impulse is 220 s;
7) Thrust misalignment angle of solid rocket motor is 0.4° (in the horizontal plane);
8) Initial transverse-roll angle is 20°;
9) With indirect fixed-depth control (pitch attitude control mode);
10) Conversion time of limit rudder angle of the head rudder is 20 ms;
11) Sampling period of pitch attitude control is 240 ms.

Simulation results of vehicle behavior can be obtained. The speed and range are shown in Fig. 10. And attack angle and pitch attitude are shown in Fig. 11.

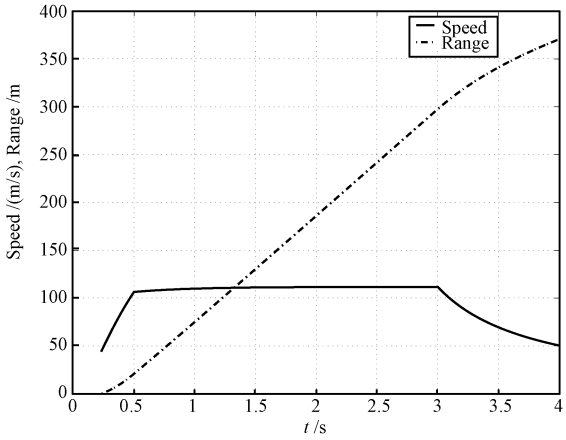

Fig. 10 Speed and range

The results show that pitch attitude increases with time, but the head rudder controller restrains the tendency of dive.

The system lag caused by too slow a response of the head rudder drive machine enlarges the overshoot and dithering.

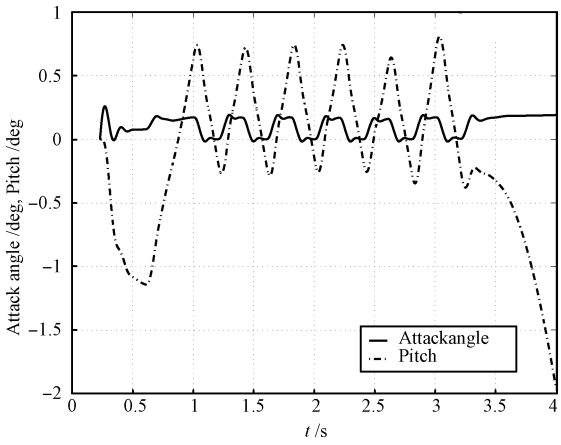

Fig. 11 Attack angle and pitch attitude

5 Experiment

To validate the control-algorithm designed, experiments have been carried out. Experimental results are shown in Fig. 12.

The results show that depth of vehicle follows up attack angle. Action command from the head rudder controller responds rapidly, which restrains the vehicle to dive.

The system stability has been intensified consumedly. The security can be ensured. The superiority of the control method is proved by the experiments. The system constitution and control algorithm are simple and well implemented.

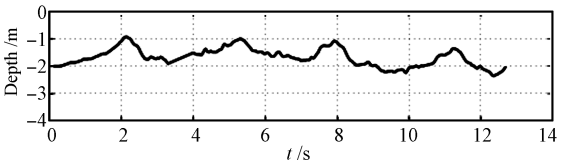

(a) Depth

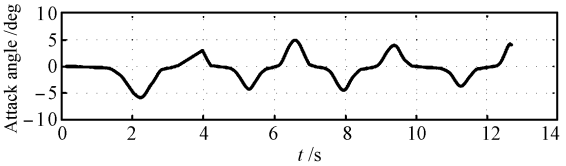

(b) Attack angle

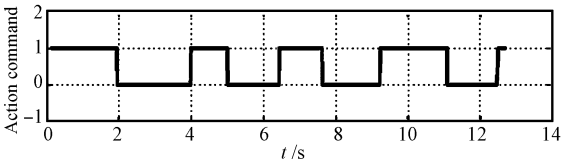

(c) Action command

Fig. 12 Experimental results

6 Conclusion

The conclusion obtained from the above analysis as follows: 1) The simple control algorithm should be designed to enlarge the sampling frequency for the stability of super-

cavitating vehicle motion characteristics on vertical plane; 2) Under the condition of lack of damp, attention should be paid to that attack angle must not exceed the limit restrictions in control process and the control force cannot be too violent; 3) A good control quality is not easily acquired by fixed-depth control directly; 4) The lag of system caused by too slow a response of the head rudder driver enlarges the regulation overshoot and dithering.

The control algorithm described in this paper has good robust, capability, and realization. The presented results are intended to provide design guidelines to help estimating the motion stability limits for the considered vehicles. Further investigations on how to construct the basic functions and somewhat simplify the structure of the stabilizing functions, typically in high-order systems, may be needed in the future practical applications.

References

1 Ahn S S, Ruzzene M. Optimal design of cylindrical shells for enhanced buckling stability: application to supercavitating underwater vehicles. *Finite Elements in Analysis and Design*, 2006, **42**(11): 967−976

2 Dzielski J, Kurdila A. A benchmark control problem for supercavitating vehicles and an initial investigation of solutions. *Journal of Vibration and Control*, 2003, **9**(7): 791−804

3 Park Y D. Dynamic stability of a free timoshenko beam under a controlled follower force. *Journal of Sound and Vibration*, 1987, **113**(3): 407−415

4 Miller D. Supercavitation: going to war in a bubble [Online], available: http://www.janes.com, December 10, 1995

5 Ashley S. Warp-drive underwater. *Scientific American*, 2001, 70−79

6 Shabana A A. Flexible multibody dynamics: review of past and recent developments. *Multibody System Dynamics*, 1997, **1**(2): 189−222

7 Kinnas S, Fine N. Non-linear analysis of the flow around partially or super-cavitating hydrofoils by a potential based panel method. In: Proceedings of the Iabem Symposium on Boundary Integral Methods: Theory and Applications. Rome, Italy: Springer-Verlag, 1990. 289−300

8 Kirschner I N, Imas L G. Plume-supercavity interactions. In: Proceedings of the International Summer Scientific School "High-Speed Hydrodynamic". Cheboksary, Russia: Springer, 2002. 147−157

9 Barre S, Rolland J, Boitel G, Goncalves E, Fortes R F. Experiments and modeling of cavitating flows in venturi: attached sheet cavitation. *European Journal of Mechanics B: Fluids*, 2009, **28**(3): 444−464

10 Semenenko V N. Dynamic processes of supercavitation and computer simulation. In: Proceedings of RTO AVT Lecture Series on "Super-Cavitating Flows". Brussels, Belgium: Von Karman Institute, 2001. 1−29

11 Choi J Y, Ruzzene M. Stability analysis of supercavitating underwater vehicles with adaptive cavitator. *International Journal of Mechanical Sciences*, 2006, **48**(12): 1360−1370

12 Kirschner I N, Kring D C, Stokes A W, Fine N E, Uhlman J S. Control strategies for supercavitating vehicles. *Journal of Vibration and Control*, 2002, **8**(2): 219−242

13 Semenenko V N. Instability of a plane ventilated supercavity in a free jet. *Prykladna Gidromehanika*, 1999, **1**(2): 45−52

14 Liu Yun-Gang. Output-feedback adaptive control for a class of nonlinear system with unknown control directions. *Acta Automatica Sinica*, 2007, **33**(12): 1306−1312

15 Chen Yan-Yan, Luo Kai. Attitude control of superspeed underwater vehicle in vertical plane. *Computer Simulation*, 2009, **26**(1): 50−54 (in Chinese)

16 Zhu Ji-Hua, Su Yu-Min, Li Ye, Tian Yu. Integral variable structure control and simulation for near-surface moment of AUV. *Journal of System Simulation*, 2007, **19**(22): 5321−5324 (in Chinese)

17 Yu Jian-Cheng, Zhang Ai-Qun, Wang Xiao-Hui, Su Li-Juan. Direct adaptive control of underwater vehicles based on fuzzy neural networks. *Acta Automatica Sinca*, 2007, **33**(8): 840−846 (in Chinese)

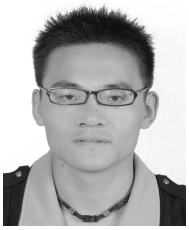

LI Dai-Jin Ph. D. candidate at the College of Marine Engineering, Northwestern Polytechnical University. His research interest covers weapon system and utilization engineering. Corresponding author of this paper. E-mail: lidaijin80@163.com

LUO Kai Received his Ph. D. degree from Northwest Polytechnical University in 1998. He is currently a professor at Northwestern Polytechnical University. His research interest covers control theory and control engineering, underwater weapon system engineering.
E-mail: luckylk@nwpu.edu.cn

ZHANG Yu-Wen Professor at Northwestern Polytechnical University. His research interest covers weapon system and utilization engineering, firing theory and technology, trajectory and control.
E-mail: zhangyuwen@nwpu.edu.cn

DANG Jian-Jun Received his Ph. D. degree from Northwestern Polytechnical University in 2004. He is now a professor at Northwestern Polytechnical University. His research interest covers weapon system and utilization engineering, and propulsion technology.
E-mail: jianjund@nwpu.edu.cn